Reaction Mechanisms

DOI: 10.1002/anie.201409844

C–H Bond Activation by Metal–Superoxo Species: What Drives High Reactivity?**

*Azaj Ansari, Prabha Jayapal, and Gopalan Rajaraman**

Abstract: *Metal–superoxo species are ubiquitous in metalloenzymes and bioinorganic chemistry and are known for their high reactivity and their ability to activate inert C–H bonds. The comparative oxidative abilities of $M–O_2^{\bullet-}$ species ($M = Cr^{III}$, Mn^{III}, Fe^{III}, and Cu^{II}) towards C–H bond activation reaction are presented. These superoxo species generated by oxygen activation are found to be aggressive oxidants compared to their high-valent metal–oxo counterparts generated by O···O bond cleavage. Our calculations illustrate the superior oxidative abilities of Fe^{III}– and Mn^{III}–superoxo species compared to the others and suggest that the reactivity may be correlated to the magnetic exchange parameter.*

Mononuclear metalloenzymes with coordinated oxygen at the metal center have applications in biology, industry, and the laboratory.[1] Oxygenated metal intermediates like oxo, peroxo, hydroperoxo, and superoxo species play a vital role in catalytic reactions such as hydrogenation, halogenation, hydroxylation, olefin epoxidation, and C–H bond activation.[2] In the last decade many high-valent metal–oxygen species have been studied to understand the fundamental structural, functional, and mechanistic aspects of their enzymes and their counterparts.[2a,d,3] Apart from the metal–oxo species, oxidation of C–H bonds by several superoxo–metal complexes is also reported.[4] Unlike the metal–oxo species, the reactivity of $M–O_2^{\bullet-}$ species and their competing oxidative abilities are relatively less explored, although nature utilizes both species to carry out efficient catalysis.[5]

Among other factors, the nature of the transition metals in $M–O_2^{\bullet-}$ species is also important, as it determines the electronic structure and the reactivity of these species. Over the years, the synthesis, structure, and reactivity of superoxo species containing copper,[6] iron,[5,7] and manganese[8] have been reported along with other metals.[9] An important addition to this class is the report of the crystal structure of the end-on $Cr–O_2^{\bullet-}$ species and kinetic studies to probe its ability to perform C–H bond activation in hydrocarbons.[10]

Metal–superoxo species are generally transient in nature and are generated at the first step of the oxygen activation both in enzyme catalysis and in biomimetic chemistry.[7c,10b] As these species are key intermediates in iron and copper catalysis, it suggests that the $M–O_2^{\bullet-}$ species perhaps play a larger role as an oxidant in enzyme catalysis.[6,11] In the $M–O_2^{\bullet-}$ species the unpaired electrons on the metal and the radical center are strongly coupled and the electronic configuration of the metal ions dictates the nature of the magnetic coupling (J) and this may in turn correlate to the C–H bond activation. Here we have undertaken a detailed theoretical study to specifically address the following questions 1) probing the mechanism of C–H bond activation by $Cr–O_2^{\bullet-}$ and its comparative oxidative ability to high-valent metal–oxo species, 2) establishing the comparative oxidative abilities of Fe^{III}, Mn^{III}, Cu^{II}, and Cr^{III} superoxo–species towards C–H bond activation reactions, and 3) elucidating the role of magnetic exchange coupling on the activation barrier.

We begin with the recently reported $[Cr(14\text{-TMC})(OO)(Cl)]^+$ (**1**; TMC = 1,4,8,11-tetramethyl-1,4,8,11-tetraazacyclotetradecane) species[10a] and elaborate later its reactivity (see Table S1 and Figures S1–S5 in the Supporting Information for computational details). The spin states play an important role in the reactivity and as a result of the radical character of the O_2 moiety, there is a direct magnetic exchange between the Cr^{III} and $O_2^{\bullet-}$ moiety. The magnetic exchange interaction between $O_2^{\bullet-}$ and the Cr^{III} ion is computed to be antiferromagnetic in nature ($-1176.3\ cm^{-1}$) and this suggests a triplet ground state for this species.[12] For this species a strong π-type interaction between the $Cr(d_{xz})$ and the oxygen π* orbital, and a relatively weak interaction between the $Cr(d_{xy})$ and oxygen π* orbital are estimated. These interactions are essentially a result of the nonlinear Cr^{III}-O-O bond angle, and the non-orthogonality and strong mixing lead to a relatively strong antiferromagnetic interaction. As we move from Cr^{III} to Mn^{III} ($[Mn(14\text{-TMC})(OO)(Cl)]^+$; **2**), Fe^{III} ($[Fe(14\text{-TMC})(OO)(Cl)]^+$; **3**), and Cu^{II} ($[Cu(14\text{-TMC})(OO)(Cl)]$; **4**),[13] the additional electrons enter into the σ* e_g (specifically $d_{z^2}/d_{x^2-y^2}$) orbitals, thus leading to orbital orthogonality and enhanced contributions to the ferromagnetic coupling. The calculated values are in line with the expectation where the computed J values are $-724.9\ cm^{-1}$, $+144.8\ cm^{-1}$, and $+299.9\ cm^{-1}$ for Mn^{III}, Fe^{III}, and Cu^{II} respectively.[14] A change in the sign of the J value leads to stabilization of $S = 3$ and $S = 1$ in the high-spin ground state for Fe^{III} and Cu^{II} superoxo–species, respectively. For $M–O_2^{\bullet-}$ type species, another important issue is the formation energies which are often not favorable.[2k,7e] In this

[*] A. Ansari, Dr. P. Jayapal, Prof. G. Rajaraman
Department of Chemistry, Indian Institute of Technology Bombay
Powai, Mumbai, Maharashtra, 400076 (India)
E-mail: rajaraman@chem.iitb.ac.in
Homepage: http://www.chem.iitb.ac.in/people/Faculty/prof/gr.html

[**] G.R. acknowledges a AISRF grant and the DST Nanomission (SR/NM/NS-1119/2011), as well as generous computational resources from IIT Bombay. A.A. thanks CSIR for a SRF fellowship.

Supporting information for this article (computational details, method assessment, tables summarizing the energetics, detailed mechanistic scheme, optimized structures and spin density plots, eigenvalue plots, orbital analysis on magnetic coupling, energies, and structures for the epoxidation reaction) is available on the WWW under http://dx.doi.org/10.1002/anie.201409844.

regard we have computed the formation energies from the $[M(14\text{-TMC})(Cl)]^{n+}$ complex, and the computed energies are exothermic in nature for all the metal ions, which suggests a favorable formation energy for this type of species (see Table S2).

We begin our study with **1**, where a detailed mechanism of C–H bond activation of 9,10-dihydroanthracene (DHA) by **1** is presented (Scheme 1) and its comparative oxidative ability with chromium–oxo counterparts such as Cr^{IV}=O and Cr^{V}=O is discussed. Then we discuss the reactivity of the

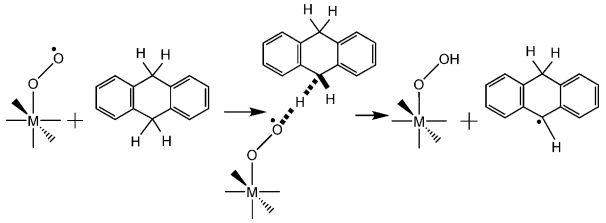

Scheme 1. Mechanism of C–H bond activation by metal–superoxo species. M = Cr^{III}, Mn^{III}, Fe^{III}, and Cu^{II}.

species **2**–**4**. DFT-computed spin-state energetics for **1** are given in Figure 1. The C–H bond activation by the superoxo species could be facilitated either by a proximal or distal oxygen atom of the $O_2^{\bullet-}$ moiety. The barrier height computed for attack by the proximal oxygen atom is prohibitively high and is related to the accessibility of the oxygen atom and the associated steric factors (supported by computed deformation energies, 49 kJ mol^{-1} versus 149 kJ mol^{-1} for the distal and proximal attacks, respectively, see below). Thus, the proximal attack results are not discussed any further.

For the distal oxygen atom attack, the barrier height is computed to be 91.7 kJ mol^{-1} (^{5}I$_d$-*ts1*) at the quintet surface while the barrier height in the triplet surface is computed to be twice as much (Figure 1). This difference demands a spin inversion[15] and suggests that the antiferromagnetic exchange observed for this species hinders its reactivity. The optimized structure of ^{5}I$_d$-*ts*1 along with the computed spin density plot is shown in Figure 2. At this transition state significant spin

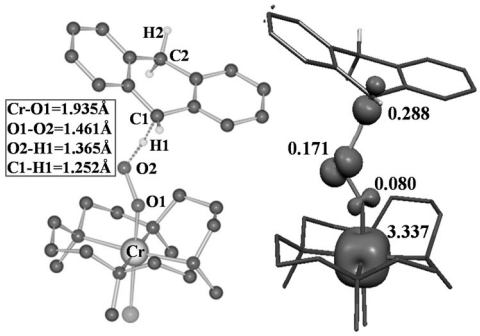

Figure 2. B3LYP-optimized structure and spin density plot of ^{5}I$_d$-*ts1*.

density on the DHA moiety is noted and this indicates a possible proton-coupled electron-transfer (PCET) mechanism for the C–H bond-activation process.[16] The abstraction of the H atom from DHA leads to the formation of Cr^{III}–OOH species and this step is exothermic by 2.0 kJ mol^{-1} (Figure 1).

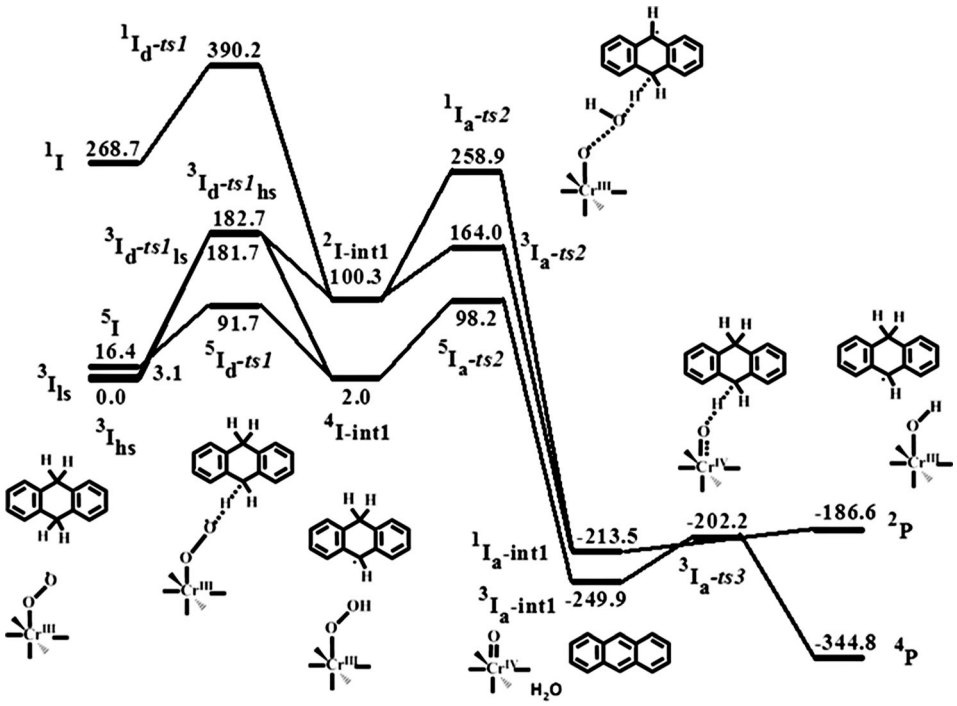

Figure 1. B3LYP-D3-computed potential energy surface (ΔG in kJ mol^{-1}) for C–H bond activation of 9,10-dihydroanthracene (DHA) by Cr^{III}–$O_2^{\bullet-}$ species.

The second hydrogen atom abstraction from the MHA (monohydroanthracene) holds the key to the formation of the final product, which is detected experimentally as a Cr^{III}–OH species.[10a] Various possible pathways for this step are illustrated in Scheme S1 in the Supporting Information. The first pathway considers abstraction of the second H atom by Cr^{III}–OOH itself, thus leading to the formation of the Cr^{IV}=O species, water, and anthracene (Pathway I$_a$; see Scheme S1 in the Supporting Information). The Cr^{IV}=O generated in this fashion could further attack another DHA and yields a Cr^{III}–OH species. The second possibility considered here is the homolytic and heterolytic (Pathway I$_b$ and I$_c$, respectively; Scheme 2) cleavage of the O··O bond of the Cr^{III}–OOH species, thus leading to the formation of

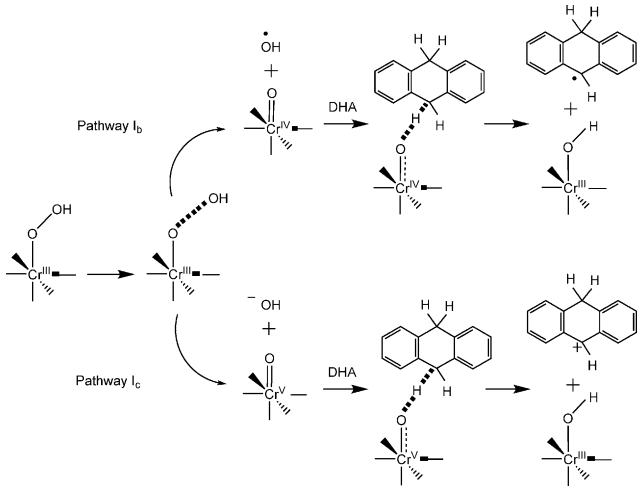

Scheme 2. Mechanism of C–H bond activation by $Cr^{IV/V}$–oxo species.

Cr^{IV}=O and Cr^{V}=O, respectively, which could then activate the second hydrogen atom.

For Pathway I_a (Figure 1), the barrier height is estimated to be 96.2 kJ mol^{-1} on the quintet surface and the formation of Cr^{IV}=O is found to be exothermic by a large energy margin.[10c] This large gain in thermodynamic stability eases further steps and eventually leads to the formation of Cr^{III}–OH species as the final product. For the Cr^{IV}=O species, the $S=1$ state is computed to be the ground state, with $S=0$ being 36.4 kJ mol^{-1} higher in energy. The computed ground state is consistent with the experimental observation, where the species is found to be EPR silent, and magnetic studies reveal an $S=1$ ground state. Calculation of the zero-field splitting parameter for this species yields a D value of -5.74 cm^{-1} with an E/D value of 0.066. The large negative D value computed is consistent with the EPR-silent nature at an X-band frequency.[10a] The unpaired electrons are found to be in the Cr(d_{xz})–O(π^*) and Cr(d_{yz})–O(π^*) orbitals with a significant spin density detected on the oxygen atom. The barrier height for the C–H bond activation by this species is 47.7 kJ mol^{-1} (Figure 1), thus indicating that this species is a stronger oxidant than the Cr^{III} superoxo species, if we ignore the energy required to generate this species. The final Cr^{III}–OH product formation is also computed to be exothermic in nature.

In the second possible pathway, the O···O bond of the Cr^{III}–OOH species is assumed to be cleaved (Scheme 2, and see Figures S6 and S7). The O···O bond of the Cr^{III}-OOH species could cleave homolytically or heterolytically (Pathway I_b or I_c; Scheme 2) and here at the transition state, the spin densities on the two oxygen atoms are equally distributed, thus suggesting an electronically favored homolytic cleavage of the O···O bond. The barrier height for this cleavage is computed to be 69.5 kJ mol^{-1} and the formation of the Cr^{IV}=O species by this pathway is also exothermic by 36.4 kJ mol^{-1}. This Cr^{IV}=O generated could attack MHA or another DHA and may finally produce a Cr^{III}–OH species. Although our transition state reveals the formation of a Cr^{IV}=O species upon O···O cleavage, an external stimuli such as protons could lead to heterolytic cleavage of the O···O bond, thus resulting in the formation of the putative Cr^{V}=O species.[2a] This species has recently been synthesized by direct oxidation of the Cr^{III} complex using iodosylbenzene as the oxidant.[10b] The Cr^{V}=O formation here from Cr^{III}–OOH, however, is excessively endothermic (183.3 kJ mol^{-1}) and suggests that Cr^{V}=O is unlikely to be generated from a Cr^{III}–OOH species without any external stimuli. Since this species has been generated by a direct oxidation route, we decided to test the C–H bond activation ability of the Cr^{V}=O species, and computed the C–H bond activation step, wherein the barrier height is estimated to be 22.1 kJ mol^{-1} and is much lower than that of the Cr^{IV}=O species. These data are in line with the nonheme iron chemistry where an Fe^{V}=O species has been termed the vigorous oxidant compared to the popular Fe^{IV}=O species.[2a,e,17]

The final product expected in the C–H bond-activation reaction is a Cr^{III}–OH species. To test also the ability of this species for C–H bond activation, we computed the corresponding transition states with DHA and also with MHA, and the computed barriers are prohibitively high (154.0 and 113.8 kJ mol^{-1}, respectively), thus suggesting product inhibition is operative in this reaction. This outcome is also in accord with ESI-MS data which suggest that the final product of this reaction is a $[Cr^{III}(14\text{-TMC})(OH)(Cl)]^+$ species.[10]

Thus, our calculations suggest that the individual oxidative abilities have the following pattern Cr^{V}=O > Cr^{IV}=O > Cr^{III}–$OO^{\bullet-}$. However if either the Cr^{IV}=O or Cr^{V}=O species are to be generated from the Cr^{III}–OOH species, the situation changes, as there is a significant kinetic barrier for the O··O bond cleavage and the calculation predicts a Cr^{III}–OO^{-} ≈ Cr^{V}=O > Cr^{IV}=O pattern for the oxidative abilities. This pattern clearly illustrates that the reaction proceeds through pathway I_a as described in Figure 1, and is supported by the oxygen-atom-transfer reaction rate reported for the superoxo species.[10b]

Now that the comparative oxidative ability within the chromium–oxo species is established, we compared the reactivity across the metal–superoxo species. The computed potential energy surfaces (PESs) for the species **1**–**4** are shown in Figure 3 (see also Figure 2). From the profile we observe that both Mn–$O_2^{\bullet-}$ and Fe–$O_2^{\bullet-}$ species have lower barrier heights, with Mn–$O_2^{\bullet-}$ possessing the lowest barrier height of all. The Cr–$O_2^{\bullet-}$ and Cu–$O_2^{\bullet-}$ species, however, possess relatively higher barrier heights, with Cu–O_2^{-} demanding close to 97.2 kJ mol^{-1} energy for the C–H bond activation. The observed trend can be rationalized based on the exchange enhanced reactivity (EER)[18] concept where lower barrier heights are expected for species possessing more unpaired electrons at the transition state. Although the EER concept predicts Fe–$O_2^{\bullet-}$ to be the lowest, the additional electron in the case of Fe enters into the $d_{x^2-y^2}$ orbital, thus rendering a weaker effective exchange. The schematic representation of orbital evolution for these species is shown in Scheme S2, and clearly demonstrates this point. These data suggest that the Fe–$O_2^{\bullet-}$ and Mn–$O_2^{\bullet-}$ species are vigorous oxidants compared to Cr–$O_2^{\bullet-}$ and Cu–$O_2^{\bullet-}$, where the computed barrier heights are much higher. To further elucidate the oxidative abilities on a different set of reactions, we tested the epoxidation of olefins (with *cis*-2-butene as

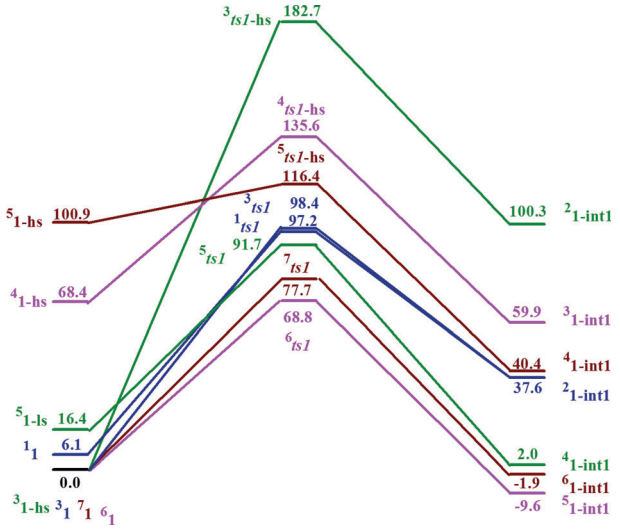

Figure 3. B3LYP-D3-computed potential energy surface (ΔG in kJ mol^{-1}) for C–H activation by chromium (green), copper (blue), iron (burgundy), and manganese (pink) superoxo species.

substrate) with these superoxo species,[19] and have computed the kinectic requirement for the epoxidation reaction. The barrier heights are estimated to be 52.6, 56.8, 76.5, and 111.8 kJ mol^{-1} for Mn–$O_2^{\bullet-}$, Fe–$O_2^{\bullet-}$, Cr–$O_2^{\bullet-}$ and Cu–$O_2^{\bullet-}$, respectively (see Figure S8 and Table S3). The trend reflected here is similar to that of the C–H activation reaction and suggests that there is a common reactivity trend among the M–$O_2^{\bullet-}$ species. This trend suggests that the reactivity pattern may have relevance to nature's choice of metal ions in metalloenzymes: choosing Fe/Mn–$O_2^{\bullet-}$ species when aggressive oxidative abilities[2f,7a,c,20] are required and Cu–O_2^{-} species when relatively milder conditions are desired.[6,7a,11]

Although the magnetic coupling among these species cannot be directly compared to the C–H bond-activation parameter, here we have probed how magnetic coupling influences these reactivities within the species. Thus, here we decided to fine-tune the *J* parameter by varying the M-O-O angle in **1**–**4** (magneto-structural correlation) and computed the barrier heights as *J* varies. A near-linear relationship between the activation barrier and *J* values are witnessed for some species (see Figure S9 and Table S4) and this reiterates our hypothesis that the magnetic coupling, which is a well-established parameter in molecular magnetism, is strongly correlated to the kinetics of the C–H bond-activation process and EER. Earlier studies on Cu–$O_2^{\bullet-}$ species[4b] and reactivity patterns associated with hemoglobin also reveal that the M-O-O angle is strongly correlated to its reactivity.[22] Since the angle alters the magnetic coupling significantly this in turn affects the reactivity. This relationship can be substantiated if the magnitudes of the spin density on the metal atoms are analyzed. Antiferromagnetic coupling resulting from delocalization/polarization of spins lead to a relatively smaller spin density compared to that of the ferromagnetic state, thus leading to larger exchange stabilization and greater reactivity. Our magneto-structural correlation suggests that structural features can be fine-tuned to alter the *J* values, which in turn will influence the reactivity of these species.

To this end, we explored the reactivity of a series of M–$O_2^{\bullet-}$ species and their competing oxidative abilities. Among different high-valent species generated by oxygen activation, metal–superoxo species are found to be the most vigorous oxidants. This reactivity is inherently due to a large kinetic barrier for the O···O bond cleavage which overshadows the strong oxidative abilities of the metal–oxo species. Among several metal-superoxo species tested, our calculations reveal that Mn/Fe–$O_2^{\bullet-}$ species are stronger oxidants compared to either Cr–$O_2^{\bullet-}$ or Cu–$O_2^{\bullet-}$, and the oxidative abilities are found to be correlated to the magnetic exchange parameter *J*. These findings have direct relevance to the functions of several metalloenzymes.

Received: October 7, 2014
Published online: November 21, 2014

Keywords: C–H activation · density functional calculations · iron · metalloenzymes · reaction mechanisms

[1] *Cytochrome P450: Structure, Mechanism, and Biochemistry* (Eds.: P. R. Ortiz de Montellano), 3rd ed, Kluwer Academic/Plenum Publishers, New York **2005**.

[2] a) A. Ansari, A. Kaushik, G. Rajaraman, *J. Am. Chem. Soc.* **2013**, *135*, 4235–4249; b) P. Comba, G. Rajaraman, H. Rohwer, *Inorg. Chem.* **2007**, *46*, 3826–3838; c) S. Shaik, H. Hirao, D. Kumar, *Acc. Chem. Res.* **2007**, *40*, 532–542; d) H. Hirao, L. Que, Jr., W. Nam, S. Shaik, *Chem. Eur. J.* **2008**, *14*, 1740–1756; e) A. Ansari, G. Rajaraman, *Phys. Chem. Chem. Phys.* **2014**, *16*, 14601–14613; f) Y.-M. Lee, S. Hong, Y. Morimoto, W. Shin, S. Fukuzumi, W. Nam, *J. Am. Chem. Soc.* **2010**, *132*, 10668–10670; g) I. Prat, J. S. Mathieson, M. Guell, X. Ribas, J. M. Luis, L. Cronin, M. Costas, *Nat. Chem.* **2011**, *3*, 788–793; h) O. V. Makhlynets, P. Das, S. Taktak, M. Flook, R. Mas-Balleste, E. V. Rybak-Akimova, L. Que, Jr., *Chem. Eur. J.* **2009**, *15*, 13171–13180; i) J. Cho, S. Jeon, S. A. Wilson, L. V. Liu, E. A. Kang, J. J. Braymer, M. H. Lim, B. Hedman, K. O. Hodgson, J. S. Valentine, E. I. Solomon, W. Nam, *Nature* **2011**, *478*, 502–505; j) P. Comba, Y. M. Lee, W. Nam, A. Waleska, *Chem. Commun.* **2014**, *50*, 412–414; k) Y. M. Badiei, M. A. Siegler, D. P. Goldberg, *J. Am. Chem. Soc.* **2011**, *133*, 1274–1277.

[3] a) J. Cho, J. Woo, J. E. Han, M. Kubo, T. Ogura, W. Nam, *Chem. Sci.* **2011**, *2*, 2057–2062; b) S. Shaik, S. Cohen, S. P. de Visser, P. K. Sharma, D. Kumar, S. Kozuch, F. Ogliaro, D. Danovich, *Eur. J. Inorg. Chem.* **2004**, 207–226; c) D. Kumar, E. Derat, A. M. Khenkin, R. Neumann, S. Shaik, *J. Am. Chem. Soc.* **2005**, *127*, 17712–17718.

[4] a) S. T. Prigge, B. A. Eipper, R. E. Mains, L. M. Amze, *Science* **2004**, *304*, 864–867; b) P. Chen, E. I. Solomon, *Proc. Natl. Acad. Sci. USA* **2004**, *101*, 13105–13110; c) E. M. Cora, A. P. Golombek, V. G. Young, Jr., C. Yang, K. Kuczera, M. P. Hendrich, A. S. Borovik, *Science* **2000**, *289*, 938–941; d) C. M. Bathelt, L. Ridder, A. J. Mulholland, J. N. Harvey, *J. Am. Chem. Soc.* **2003**, *125*, 15004–15005; e) C. M. Bathelt, L. Ridder, A. J. Mulholland, J. N. Harvey, *Org. Biomol. Chem.* **2004**, *2*, 2998–3005.

[5] K. Cho, H. Chen, D. Janardanan, S. P. de Visser, S. Shaik, W. Nam, *Chem. Commun.* **2012**, *48*, 2189–2191.

[6] D. Maiti, H. C. Fry, J. S. Woertink, M. A. Vance, E. I. Solomon, K. D. Karlin, *J. Am. Chem. Soc.* **2007**, *129*, 264–265.

[7] a) H. Chen, K.-B. Cho, W. Lai, W. Nam, S. Shaik, *J. Chem. Theory Comput.* **2012**, *8*, 915 – 926; b) K. Duerr, J. Olah, R. Davydov, M. Kleimann, J. Li, N. Lang, R. Puchta, E. H. Hubner, T. Drewello, J. N. Harvey, N. Juxa, I. Ivanovic-Burmazovic, *Dalton Trans.* **2010**, *39*, 2049 – 2056; c) L. W. Chung, X. Li, H. Hirao, K. Morokuma, *J. Am. Chem. Soc.* **2011**, *133*, 20076 – 20079; d) M. M. Mbughuni, M. Chakrabarti, J. A. Hayden, E. L. Bominaar, M. P. Hendrich, E. Munck, J. D. Lipscomb, *Proc. Natl. Acad. Sci. USA* **2010**, *107*, 16788 – 16793; e) D. Mandon, H. Jaafar, A. Thibon, *New J. Chem.* **2011**, *35*, 1986 – 2000.

[8] J. W. Egan, B. S. Haggerty, A. L. Rheingold, S. C. Sendlinger, K. H. Theopold, *J. Am. Chem. Soc.* **1990**, *112*, 2445 – 2446.

[9] a) M. S. Seo, J. Y. Kim, J. Annaraj, Y. Kim, Y.-M. Lee, S.-J. Kim, J. Kim, W. Nam, *Angew. Chem. Int. Ed.* **2007**, *46*, 377 – 380; *Angew. Chem.* **2007**, *119*, 381 – 384; b) V. N. Shetti, M. J. Rani, D. Srinivas, P. Ratnasamy, *J. Phys. Chem. B* **2006**, *110*, 677 – 679; c) J. Cho, H. Y. Kang, L. V. Liu, R. Sarangi, E. I. Solomon, W. Nam, *Chem. Sci.* **2013**, *4*, 1502 – 1508.

[10] a) J. Cho, J. Woo, W. Nam, *J. Am. Chem. Soc.* **2010**, *132*, 5958 – 5959; b) J. Cho, J. Woo, W. Nam, *J. Am. Chem. Soc.* **2012**, *134*, 11112 – 11115; c) K.-B. Cho, H. Kang, J. Woo, Y. J. Park, M. S. Seo, J. Cho, W. Nam, *Inorg. Chem.* **2014**, *53*, 645 – 652; d) A. Yokoyama, K. B. Cho, K. D. Karlin, W. Nam, *J. Am. Chem. Soc.* **2013**, *135*, 14900 – 14903.

[11] a) D. Maiti, D.-H. Lee, K. Gaoutchenova, C. Würtele, M. C. Holthausen, A. A. N. Sarjeant, J. Sundermeyer, S. Schindler, K. D. Karlin, *Angew. Chem. Int. Ed.* **2008**, *47*, 82 – 85; *Angew. Chem.* **2008**, *120*, 88 – 91.

[12] a) S. Tewary, I. A. Gass, K. S. Murray, G. Rajaraman, *Eur. J. Inorg. Chem.* **2013**, 1024 – 1032; b) J. Cano, E. Ruiz, S. Alvarez, M. Verdaguer, *Comments Inorg. Chem.* **1998**, *20*, 27 – 56; c) E. Ruiz, S. Alvarez, A. Rodriguez-Fortea, P. Alemany, Y. Pouillon, C. Massobrio in *Magnetism: Molecules to Materials* (Eds.; J. S. Miller, M. Drillon), Wiley-VCH, Weinheim New York, **2001**, *Vol. II*, pp. 227 – 279.

[13] Consistency calculations are done on $[M(14\text{-TMC})(OO)(Cl)]^{n+}$ models with $M = Mn^{III}$, Fe^{III}, and Cu^{II}.

[14] To make the comparison straight forward, calculation of the Fe– and Cu–superoxo complexes have also been performed with the 14-TMC ligand and an axial chlorine atom.

[15] J. N. Harvey, M. Aschi, H. Schwarz, W. Koch, *Theor. Chem. Acc.* **1998**, *99*, 95 – 99.

[16] a) M. Jaccob, A. Ansari, B. Pandey, G. Rajaraman, *Dalton Trans.* **2013**, *42*, 16518 – 16526; b) J. J. Warren, T. A. Tronic, J. M. Mayer, *Chem. Rev.* **2010**, *110*, 6961 – 7001.

[17] A. Bassan, M. R. A. Blomberg, P. E. M. Siegbahn, L. Que, Jr., *J. Am. Chem. Soc.* **2002**, *124*, 11056 – 11063.

[18] S. Shaik, H. Chen, D. Janardanan, *Nat. Chem.* **2011**, *3*, 19 – 27.

[19] J. M. Bollinger, Jr., C. Krebs, *Curr. Opin. Chem. Biol.* **2007**, *11*, 151 – 158.

[20] A. Mukherjee, M. A. Cranswick, M. Chakrabarti, T. K. Paine, K. Fujisawa, E. Munck, L. Que, Jr., *Inorg. Chem.* **2010**, *49*, 3618 – 3628.

[21] a) R. L. Peterson, R. A. Himes, H. Kotani, T. Suenobu, L. Tian, M. A. Siegler, E. I. Solomon, S. Fukuzumi, K. D. Karlin, *J. Am. Chem. Soc.* **2011**, *133*, 1702 – 1705; b) A. Kunishita, M. Kubo, H. Sugimoto, T. Ogura, K. Sato, T. Takui, S. Itoh, *J. Am. Chem. Soc.* **2009**, *131*, 2788 – 2789; c) C. J. Cramer, W. B. Tolman, *Acc. Chem. Res.* **2007**, *40*, 601 – 608; d) C. Würtele, E. Gaoutchenova, K. Harms, M. C. Holthausen, J. Sundermeyer, S. Schindler, *Angew. Chem. Int. Ed.* **2006**, *45*, 3867 – 3869; *Angew. Chem.* **2006**, *118*, 3951 – 3954; e) S. Itoh, *Curr. Opin. Chem. Biol.* **2006**, *10*, 115 – 122.

[22] a) G. B. Jameson, G. A. Rodley, W. T. Robinson, R. R. Gagne, C. A. Reed, J. P. Collman, *Inorg. Chem.* **1978**, *17*, 850 – 857; b) R. Hoffmann, M. M. L. Chen, D. L. Thorn, *Inorg. Chem.* **1977**, *16*, 503 – 511; c) R. F. Kirchner, G. H. Loew, *J. Am. Chem. Soc.* **1977**, *99*, 4639 – 4647.

